JOURNAL OF APPLIED ELECTROCHEMISTRY 17 (1987) 1177–1189

Mass transfer at gas-evolving vertical electrodes

L. J. J. JANSSEN

Laboratory for Electrochemistry, Department of Chemical Technology, Eindhoven University of Technology, PO Box 513, 5600 MB Eindhoven, The Netherlands

Received 27 January 1987; revised 26 April 1987

Various models have been proposed to describe the mass transfer of indicator ions to gas-evolving electrodes. For verification of the proposed models, the dependence of the mass transfer coefficient of indicator ions, k_j, on the length, L_e, of a gas-evolving electrode may be very useful. Experimental relations between k_j and L_e have been determined for oxygen-evolving as well as hydrogen-evolving vertical electrodes in a supporting electrolyte of 1 M KOH. Moreover, a modified hydrodynamic model, where a laminar solution flow is induced by rising bubbles, has been proposed in order to calculate k_j. It has been found that this model is not useful for both types of gas-evolving electrodes. The experimental results support the earlier proposed convection–penetration model for the oxygen-evolving electrode. The solution flow near a vertical electrode, induced by rising bubbles, behaves in a turbulent manner.

Nomenclature

A_e	electrode surface area
A_1	parameter defined by Equation 13
A_2	parameter defined by Equation 14
A_3	A_1/A_2
A_4	parameter defined by Equation 34
c	concentration
c^s	concentration in bulk of solution
D	diffusion coefficient
d_e	equivalent diameter of cell compartment at the level of the working electrode
F	Faraday constant
F_B	buoyant force
F_S	shear force
g	acceleration due to gravity
i	current density
k_j	mass transfer coefficient of indicator ion j to an electrode
L_e	length of electrode
m	parameter defined by Equation 13
m_j	quantity of species j
M	momentum flow
ΔM	change in M
n	parameter defined by Equation 13
p	parameter, $x^{3/4}$
v	velocity of solution flow
v^s	velocity of bulk solution flow
v_1	v defined by Equation 2
V_B	volume of bubbles
w	width of a volume element
x	coordinate, distance from leading edge of electrode
y	coordinate, distance to the electrode
z	coordinate, width of electrode
δ	boundary layer thickness
δ_b	bubble layer thickness at the electrode
δ_n	Nernst diffusion layer thickness
ε	gas voidage
ϱ	density
ϱ_{av}	average density of a mixture of solution and bubbles in a volume element
ϱ_s	density of bulk solution
ϱ_g	density of gas
μ	viscosity
μ_w	viscosity of solution–gas bubble mixture at the electrode surface
ν	kinematic viscosity, $\nu = \mu/\varrho$
ψ	parameter defined by Equation 26

Subscripts

av	average
b	bubble layer at the surface of electrode
B	bubble-induced convection
e	electrode
F	forced convection

0021–891X/87 $03.00 + .12

fi	$Fe(CN)_6^{3-}$	max	maximum
fo	$Fe(CN)_6^{4-}$	N	natural convection
FB	combined forced and bubble-induced convection	s	bulk of solution
		w	on the electrode surface
g	gas		

1. Introduction

Mass transfer at gas-evolving electrodes is one of the most important topics in applied electrochemistry. In particular, the mass transfer of indicator ions to a gas-evolving electrode has been extensively studied. Vogt [1] has published a recent survey.

Different models have been presented to describe the mass transfer coefficient, k_j, of the indicator, j, to a gas-evolving electrode in the presence or absence of forced convection of solution. The usefulness of the various models depends to a considerable extent on the occurrence or non-occurrence of coalescence of the bubbles formed during gas evolution [2]. A penetration model [3] and a convection–penetration model [2] are very suitable for a gas-evolving electrode with coalescing bubbles, e.g. the oxygen-evolving electrode in alkaline solution, in natural convection as well as combined forced and natural convection. For a gas-evolving electrode, where practically no coalescence of bubbles occurs, e.g. the hydrogen-evolving electrode in alkaline solution, a hydrodynamic model has been proposed for natural convection [4, 5]. A quantitative description of this model – given for a horizontal gas-evolving electrode – has been based on an empirical relation for turbulent flow caused by differences in density of the solution [4].

In this paper, a modified hydrodynamic model is presented to describe the mass transfer of indicator ions to a vertical gas-evolving electrode. To check the relations deduced, measurements of mass transfer coefficients have been carried out for electrodes with different lengths in combined forced and natural convection.

2. Experimental details

The electrolytic cell used for all measurements was a two-compartment Perspex cell; the compartments were separated by a cation-exchange membrane (Nafion, Type 427). The cell is sketched in Fig. 1. Both compartments consisted of three parts; the middle one was rectangular, its width being 20 mm and its length 220 mm. The distance between the membrane and the working electrode was 10 mm. The working electrode was placed against the centre of the back wall of the working electrode compartment. Nickel plate electrodes of various lengths, namely 5, 10, 20, 40, 80 and 160 mm, were used as the working electrode. The counter electrode was an expanded metal–nickel gauze of dimensions 20 × 16 mm and was pressed against the membrane directly opposite the working electrode. Solution was pumped through each compartment of the cell; the two solution-flow circuits were similar to those described in [6]. The initial volume of solution in the flow circuits with the working electrode depended on electrolytic conditions and was varied between 1500 and 3000 cm^3.

Before starting a series of mass transfer measurements, a pre-electrolysis was carried out in 1 M KOH for 20 min at the highest current density applied during the series of mass transfer experiments. The current was switched off and a 1 M KOH solution containing a fixed quantity of indicator ions was added to the 1 M KOH solution in the working electrode flow circuit. $Fe(CN)_6^{3-}$ was used as the indicator ion for oxygen evolution and also in the absence of gas evolution, and $Fe(CN)_6^{3-}$ was used for hydrogen evolution. The initial indicator concentration was 0.05 M. After homogenizing the solution, the electrolysis was carried out at a constant current, in most cases for 90 min. After each period of 15 min a 15 cm^3 sample was taken for analysis of the solution. Unlike the procedures in previous research, the concentration of $Fe(CN)_6^{3-}$ and of $Fe(CN)_6^{4-}$ was determined

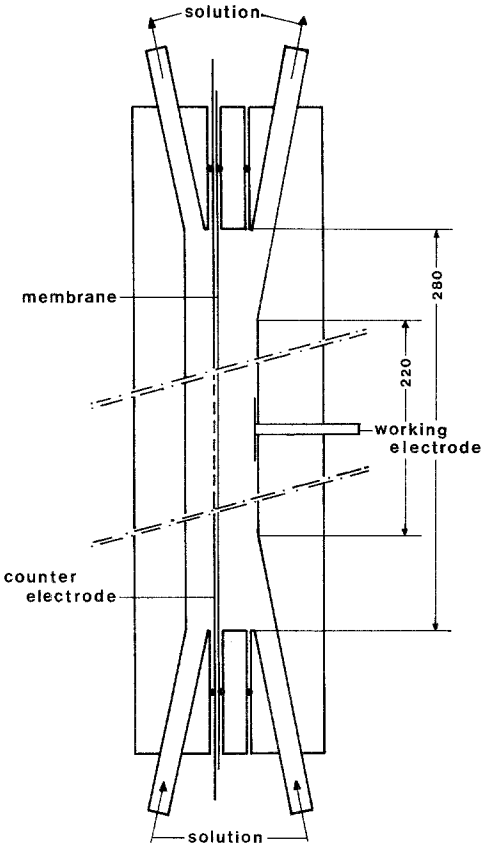

Fig. 1. Electrolytic cell.

from the limiting current occurring in the voltammetric curves for a rotating platinum disc electrode with a surface area of 0.55 cm^2, a rotating speed of 64 s^{-1} and at a potential scan rate of 0.1 V s^{-1}.

The limiting current of $Fe(CN)_6^{3-}$ reduction occurred at -0.5 V versus SCE and that of $Fe(CN)_6^{4-}$ oxidation at 0.45 V versus SCE. The proportional factor between the limiting current of $Fe(CN)_6^{4-}$ oxidation, $i_{g,fo}$, and the $Fe(CN)_6^{4-}$ concentration in the bulk, c_{fo}^s, and that between the limiting current of $Fe(CN)_6^{3-}$ reduction, $i_{g,fi}$, and the $Fe(CN)_6^{3-}$ concentration in the bulk, c_{fi}^s, were determined by calibration. Taking into account the volume of solution in the flow circuit of the working electrode, the quantity of the indicator ion, m_j, reduced or oxidized during the electrolysis, was obtained as a function of the time of electrolysis, t_e. Generally, the m_j/t_e function can be represented by a straight line.

The mass transfer coefficient for the indicator ion, k_j, was calculated from the slope of the m_j/t_e straight and the average concentration of the indicator ion during the period of electrolysis.

Despite the continuous decrease in the concentration of the indicator ion with the time of electrolysis, it was found that its average concentration was a reliable approach to the calculation of k_j.

3. Experimental results

3.1. *Mass transfer to an electrode in the absence of gas evolution*

In alkaline solution, $Fe(CN)_6^{3-}$ is usually used as an indicator ion to determine mass transfer to electrodes. The potential–current density curve for a nickel electrode in 1 M KOH + 0.05 M

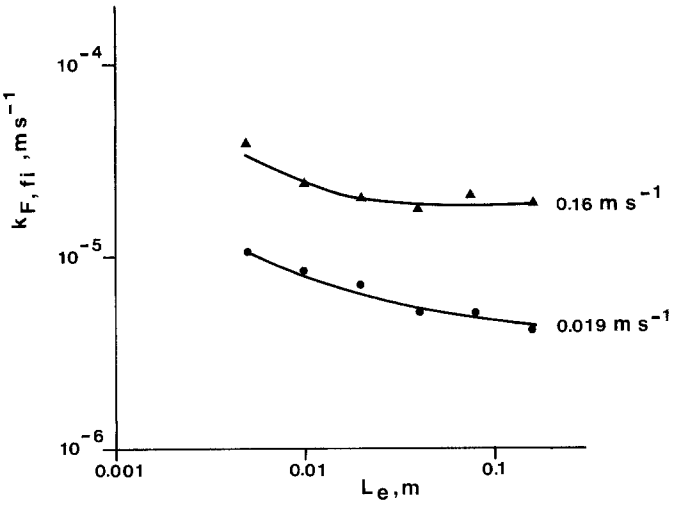

Fig. 2. Mass transfer coefficient of ferricyanide ions to an electrode at forced convection and in absence of gas evolution as a function of the length of electrode on a double logarithmic scale.

$K_3Fe(CN)_6$ and at 298 K showed a limiting current region from -0.2 to -1.4 V versus SCE for the reduction of $Fe(CN)_6^{3-}$. The mass transfer coefficient for $Fe(CN)_6^{3-}$, k_{fi}, was calculated from the well-known relation

$$k_{fi} = i_{fi}/Fc_{fi}^{s}$$

where i_{fi} is the limiting current density for the reduction of $Fe(CN)_6^{3-}$ to $Fe(CN)_6^{4-}$, and c_{fi}^{s} is the concentration of $Fe(CN)_6^{3-}$ in the bulk solution.

For forced convection and in the absence of gas-bubble evolution, k_{fi} is indicated by $k_{F,fi}$. It has been found that for nickel electrodes with lengths from 0.005 to 0.16 m at a solution flow velocity from 0.09 to 0.16 m s^{-1}, $k_{F,fi}$ is proportional to v^{a_1} where a_1 depends slightly on L_e, for instance $a_1 = 0.66$ for $L_e = 0.05$ m and $a_1 = 0.80$ for $L_e = 0.16$ m. The effect of L_e on $k_{F,fi}$ is given in Fig. 2 for both a low and a high solution velocity i.e. 0.019 and 0.16 m s^{-1}. Fig. 2 shows that $k_{F,fi}$ decreases at a decreasing rate with increasing L_e. The decrease in $k_{F,fi}$ for $L_e > 0.02$ m is smaller for $v_s = 0.16$ m s^{-1} than that for $v_s = 0.019$ m s^{-1}.

3.2. *Mass transfer to a gas-evolving electrode with forced convection*

The mass transfer coefficient of $Fe(CN)_6^{3-}$, k_{fi}, to a hydrogen-evolving electrode and that of $Fe(CN)_6^{4-}$, k_{fo}, to an oxygen-evolving electrode were determined at two different velocities of solution, namely 0.019 and 0.16 m s^{-1}, and at two different current densities, namely 0.47 and

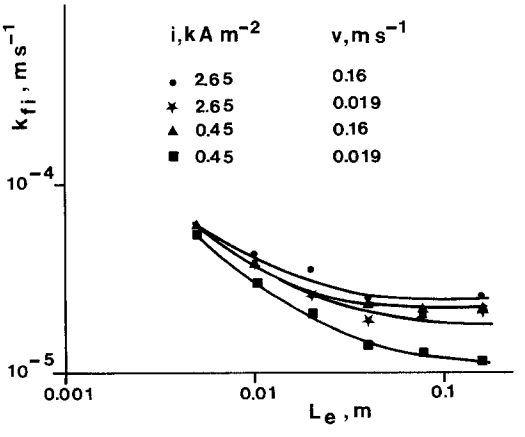

Fig. 3. Mass transfer coefficient of ferricyanide ions to a hydrogen-evolving electrode at forced convection as a function of the length of electrode on a double logarithmic scale at various current densities for hydrogen evolution and at various velocities of solution flow.

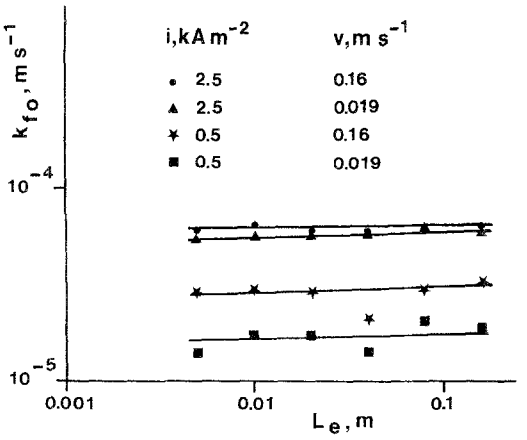

Fig. 4. Mass transfer coefficient of ferrocyanide ions to an oxygen-evolving electrode at forced convection as a function of the length of electrode on a double logarithmic scale at various current densities for oxygen evolution and at various velocities of solution flow.

2.9 mA m^{-2}. The ratios i_H/i_{fi} and i_0/i_{fo} at a constant current density decreased with increasing length of electrode. To obtain k_{fi} and k_{fo} for electrodes with different lengths at a constant rate of gas evolution, the k_{fi}/i_H and k_{fo}/i_0 curves were interpolated or linearly extrapolated. This procedure is justified by the results given in [6].

Fig. 3 shows the dependence of k_{fi} on L_e for a hydrogen-evolving electrode at $v_s = 0.019$ and 0.16 m s^{-1} and $i_H = 0.45$ and 2.65 kA m^{-2}. Results for oxygen-evolving electrodes are given in Fig. 4. By linear extrapolation of the k_{fi}/v_s curve at a constant rate of hydrogen evolution, the mass transfer coefficient for $Fe(CN)_6^{3-}$, $k_{B,fi}$, was obtained in the absence of forced convection. This extrapolation is reasonable in view of the results of [6].

In Fig. 5, $k_{B,fi}$ is plotted versus L_e on a double logarithmic scale for hydrogen evolution with $i_H = 0.5$ and 2.7 kA cm^{-2} and at $v_s = 0.019$ and 0.16 m s^{-1}. From Figs 3 and 5 it follows that the shape of the log $k_{B,fo}$/log L_e curve is similar to that of the log k_{fo}/log L_e curve. Fig. 4 shows that for an oxygen-evolving electrode, k_{fo} is practically independent of L_e, so that $k_{B,fo}$ is also practically independent of L_e.

4. Theory

4.1. *Bubble layer at a gas-evolving vertical electrode under bubble-induced convection*

A boundary layer containing rising bubbles – the bubble layer – is formed at a gas-evolving vertical electrode. By analogy with the solution flow caused by changes in density of the solution within the boundary layer at a vertical electrode during current flow [7] or at a heated vertical plate [8], it is assumed that the stream lines of the solution flow in the vicinity of the gas-evolving vertical electrode in steady state conditions are directed vertically. The solution flow is caused by rising

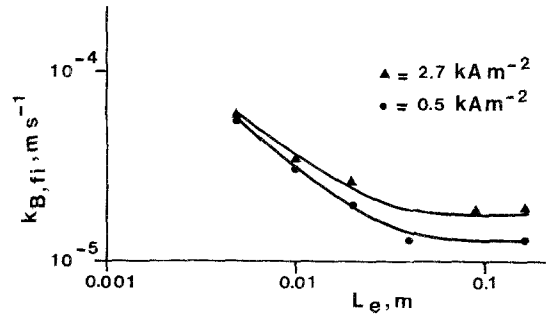

Fig. 5. Mass transfer coefficient of ferricyanide ions to a hydrogen-evolving electrode in the absence of forced convection as a function of the length of electrode on a double logarithmic scale at two current densities for hydrogen evolution.

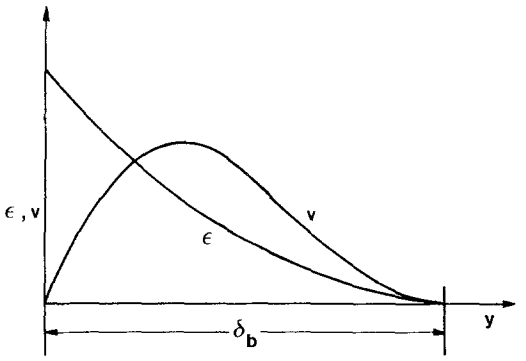

Fig. 6. Flow velocity and gas voidage profile in natural convection.

bubbles within the bubble layer. The thickness of the bubble layer, δ_b, increases in the vertical direction (x direction).

In the steady state, ε is approximated by

$$\varepsilon = \varepsilon_w(1 - y/\delta_b)^2 \tag{1}$$

and the solution velocity by

$$v = v_1 y/\delta_b(1 - y/\delta_b)^2 \tag{2}$$

The gas voidage, ε, as a function of the distance y from a hydrogen-evolving electrode has been determined by Bongenaar-Schlenter *et al.* [9]. It has been found that Equation 1 is useful in describing the profile of gas voidage. The distribution for ε and v within the bubble layer is shown in Fig. 6. Analogous cases of heat transfer [8] and mass transfer [7] have been studied under steady-state free convection.

The bubble-layer thickness for the gas voidage and solution flow velocity profiles is set equal because the solution flow is only generated by rising bubbles. The maximum velocity, v_{max}, occurs at $y = \delta_b/3$ and is $0.148v_1$ [8]. To derive a theoretical relation for δ_b the solution flow velocity is considered to be only a function of the x and y coordinates. For the volume element of height dx and width w, the buoyant force, F_B, relative to ϱ_s, is

$$F_B = dx \int_0^w (\varrho - \varrho_s) g \, dy \tag{3}$$

For a mixture of solution and bubbles, and assuming $\varrho_g \ll \varrho_s$, it can be deduced that

$$\varrho - \varrho_s = -\varepsilon\varrho_s \tag{4}$$

Introduction of Equation 4 into Equation 3 gives an upwards-directed force,

$$F_B = -dx\,\varrho_s g \int_0^w \varepsilon \, dy \tag{5}$$

Because of the solution velocity gradient, a shear stress acts downwards on the solution element at the wall. For the volume element of height dx and width w, the resulting shear force F_S is given by

$$F_S = \mu_w \left(\frac{dv}{dy}\right)_w \tag{6}$$

Since the pressure is constant in the bubble layer (because of the low velocities) and the velocity at the edge of the bubble layer is zero, the change in momentum, ΔM, over the element with a height dx and width w is

$$\Delta M = \varrho_{av} \int_0^h v^2 \, dy \tag{7}$$

where ϱ_{av} is the average density of the mixture of solution and bubbles for the element.

Using the general momentum equation and introducing the various terms into this equation, it

can be shown that

$$\varrho_{av} \frac{d}{dx} \int_0^h v^2 \, dy = \varrho_s g \int_0^h \varepsilon \, dy - \mu_w \left(\frac{dv}{dy}\right)_w \tag{8}$$

Since $\varrho_g \ll \varrho_s$ then $\varrho_{av} = (1 - \varepsilon_{av})\varrho_s$.

This integral equation is simplified assuming $\mu_w = (1 + 2.5\varepsilon_w)\mu_s$ (bubbles are considered as rigid spheres [10]) and $\varrho_{av} = (1 - \varepsilon_{av})\varrho_s$. From Equation 1 it follows that $\varepsilon_{av} = \varepsilon_w/3$, so that $\varrho_{av} = (1 - \varepsilon_w/3)\varrho_s$. Since $\mu_s = \varrho_s \nu_s$, substitution of ϱ_{av} and μ_w, after rearrangement, gives

$$\frac{d}{dx} \int_0^h v^2 \, dy = \frac{g}{1 - 0.33\varepsilon_w} \int_0^h \varepsilon \, dy - \frac{1 + 2.5\varepsilon_w}{1 - 0.33\varepsilon_w} \nu_s \left(\frac{dv}{dy}\right)_w \tag{9}$$

For the gas voidage and velocity profiles shown by Equations 1 and 2, respectively, according to [8], we obtain

$$\int_0^h \varepsilon \, dy = \varepsilon_w \delta/3 \tag{10}$$

and

$$\int_0^h v^2 \, dy = v_l^2 \delta_b/105 \tag{11}$$

Introducing Equations 10 and 11 into Equation 9 gives

$$\frac{1}{105}\left(\frac{d}{dx}\right)(v_l^2 \delta_b) = \frac{g\varepsilon_w \delta_b}{3 - \varepsilon_w} - \frac{1 + 2.5\varepsilon_w}{1 - 0.33\varepsilon_w} \nu_s \left(\frac{v_l}{\delta_b}\right) \tag{12}$$

We will attempt to determine whether power functions for the velocity and the bubble layer thickness satisfy Equation 12 so that

$$v_l = A_1 x^m \tag{13}$$

and

$$\delta_b = A_2 x^n \tag{14}$$

These relations are introduced into Equation 12. The resulting equation must be valid for arbitrary values of x; thus for this equation the exponent of x has the same value of each term. It can be shown that $m = 1/2$ and $n = 1/4$ [8].

When these numerical values are substituted in Equation 12, it follows that

$$\frac{A_1^2 A_2}{84} = \frac{g\varepsilon_w A_2}{3 - \varepsilon_w} - \frac{1 + 2.5\varepsilon_w A_1 \nu_s}{1 - 0.33\varepsilon_w A_2} \tag{15}$$

From Equation 15 the parameters A_1 and A_2 cannot be obtained separately. Therefore, additional information is necessary. Substitution of Equation 14 and $n = 1/4$ into Equation 1 gives

$$\varepsilon = \varepsilon_w (1 - y/A_2 x^{1/4})^2 \tag{16}$$

The volume of bubbles in the bubble layer is given by

$$V_{B,b} = \int_0^{H_e} \int_0^{\delta_b} \varepsilon_w \left(1 - \frac{y}{A_2 x^{1/4}}\right)^2 dy \, dx \tag{17}$$

When ε_w and $V_{B,b}$ are known, the parameter A_2, and hence A_1, can be calculated.

Substitution of Equation 13 and $m = 1/2$ into Equation 2 gives

$$v = \frac{A_1 x^{1/4} y}{A_2} \left(1 - \frac{y}{A_2 x^{1/4}}\right)^2 \tag{18}$$

The velocity profile is given by Equation 18 and can be calculated when A_1 and A_2 are well known.

4.2. *Mass transfer at a gas-evolving vertical electrode under bubble-induced convection*

The mass transfer to a gas-evolving vertical electrode is treated as a two-dimensional problem in the x and y coordinates; this is indicated in Fig. 6. In the steady state the convective mass transfer can be given for an ionic species in the presence of excess supporting electrolyte or for an uncharged species by [11], so that

$$v_x\left(\frac{\mathrm{d}c}{\partial x}\right) + v_y\left(\frac{\partial c}{\partial y}\right) = D\left(\frac{\partial^2 c}{\partial x^2} + \frac{\partial^2 c}{\partial y^2}\right) \tag{19}$$

According to the model of Fig. 6, $v_y = 0$. Because mass transfer in the x-direction will be mainly due to convection rate than diffusion,

$$\frac{\partial^2 c}{\partial x^2} \ll \frac{\partial^2 c}{\partial y^2}.$$

An acceptable approximation to Equation 19 is given in [11] and is quoted below, namely

$$v_x\left(\frac{\partial c}{\partial x}\right) = D\left(\frac{\partial^2 c}{\partial y^2}\right) \tag{20}$$

Since the thickness of the Nernst diffusion layer $\delta \ll \delta_b$, the local velocity of solution flow close to the electrode can be approximated by a linear relation. From Equation 18 and by substituting $A_1/A_2 = A_3$ it follows that

$$v_x = A_3 x^{1/4} y \tag{21}$$

which enables Equation 20 to be simplified to

$$A_3 x^{1/4} y\left(\frac{\partial c}{\partial x}\right) = D\left(\frac{\partial^2 c}{\partial y^2}\right) \tag{22}$$

Equation 22 will be used as the basic differential relation to describe the mass transfer of indicator ions to a gas-evolving electrode. Rearrangement of Equation 22 gives

$$A_3\left(\frac{\partial c}{\partial x^{3/4}}\right) = \frac{4D\partial^2 c}{3y\partial y^2} \tag{23}$$

Substitution of $x^{3/4}$ by p into Equation 23 shows that

$$A_3\left(\frac{\partial c}{\partial p}\right) = \frac{4D\partial^2 c}{3y\partial y^2} \tag{24}$$

The boundary conditions to Equation 24 are

$$c = 0 \quad \text{at} \quad y = 0 \quad \text{for} \quad x \geqslant 0$$
$$c = c^s \quad \text{at} \quad y = \delta_b \quad \text{for} \quad x \geqslant 0$$

Equation 24 is similar to relation 4.6 from [11]. To solve this relation a combination of variables technique is used [11]. It can be shown that Equation 24 can be transformed to the ordinary differential equation [11], namely

$$\frac{\mathrm{d}^2 c}{\mathrm{d}\psi^2} + 3\psi^2 \frac{\mathrm{d}c}{\mathrm{d}\psi} = 0 \tag{25}$$

where

$$\psi = \frac{y}{p^{1/3}}\left(\frac{4A_3}{27D}\right)^{1/3} \tag{26}$$

Substitution of p by $x^{3/4}$ gives

$$\psi = \frac{y}{x^{1/4}}\left(\frac{4A_3}{27D}\right)^{1/3} \tag{27}$$

Equation 25 can be solved by successive use of integrating factors [11] to give

$$\frac{c}{c^s} = \frac{1}{0.893}\int_0^{\psi} e^{-\psi^3}\,\mathrm{d}\psi \tag{28}$$

The local mass transfer coefficient, k_x, is defined by

$$k_x = \frac{D}{c^s}\left(\frac{\mathrm{d}c}{\mathrm{d}y}\right)_{y=0} = \frac{D}{c^s}\left(\frac{\mathrm{d}c}{\mathrm{d}\psi}\right)_{\psi=0}\left(\frac{\mathrm{d}\psi}{\mathrm{d}y}\right) \tag{29}$$

Since $\mathrm{d}\psi/\mathrm{d}y$ can be obtained from Equation 26 and $(\mathrm{d}c/\mathrm{d}\psi)_{\psi=0}$ from Equation 28, it can be shown that

$$k_x = 0.59D^{2/3}A_3^{1/3}x^{-1/4} \tag{30}$$

The average mass transfer coefficient, k_{av}, over an electrode of length L_e is given by

$$k_{av} = \frac{1}{L_e}\int_0^{L_e} 0.59D^{2/3}A_3^{1/3}x^{-1/4}\,\mathrm{d}x \tag{31}$$

Hence

$$k_{av} = 0.79D^{2/3}A_3^{1/3}L_e^{-1/4} \tag{32}$$

The average mass transfer coefficient of indicator ions to a gas-evolving electrode is proportional to $L_e^{-1/4}$. The determination of both parameters A_1 and A_2 is given in the previous section.

4.3. *Mass transfer at a gas-evolving electrode with combined forced convection and gas evolution*

The problem of combined natural and forced convection in heat or mass transfer has been studied extensively [12–15] and is very complicated. To solve the transport equations, approximations are necessary. In contrast to the natural convection discussed in the literature [12–15], the convection at a gas-evolving electrode is caused by rising bubbles. For a gas-evolving electrode with forced convection of the electrolyte the mass transfer boundary layer for indicator ions is much thinner than both the bubble layer and the hydrodynamic boundary layer. It is assumed that, close to the electrode surface, within the mass transfer boundary layer, the velocity of solution flow with combined convection is approximately the sum of the velocities of forced and bubble-induced convection, as if they existed independently. Consequently, $v_x = v_{x,F} + v_{x,N}$.

In the steady state the convective mass transfer equation for a laminar flow in the x-direction is given by Equation 20. Substitution of v_x by $v_{x,F} + v_{x,N}$ into Equation 20 gives

$$(v_{x,F} + v_{x,N})\left(\frac{\partial c}{\partial x}\right) = D\left(\frac{\partial^2 c}{\partial y^2}\right) \tag{33}$$

For a developing laminar flow [16] near the electrode surface, a reasonable approach is given by

$$v_{x,F} = A_4 x^{-1/2} y \tag{34}$$

This relation is also given by Jorné [15]; however, he gives no further information about the type of solution flow.

Assuming

$$v_{x,N} = A_3 x^{1/4} y, \tag{35}$$

and from Equation 34 it can be shown that

$$(A_4 x^{-1/2} + A_3 x^{1/4}) \left(\frac{\partial c}{\partial x}\right) = \frac{D\partial^2 c}{y\partial y^2} \tag{36}$$

We discuss here the case in which the solution flow is laminar and the flow-stream lines for the combined flow are parallel to the x-direction (Fig. 6). The boundary conditions are

$$v_x = 0 \quad \text{and} \quad c = 0 \quad \text{at} \quad y = 0$$

$$v_x = v^s, \quad c = c^s \quad \text{at} \quad y = \infty$$

$$v_x = v^s, \quad c = c^s \quad \text{at} \quad x = 0.$$

Equation 33 has been dissolved by Jorné [15] for the boundary conditions mentioned. The resultant local mass transfer coefficient [15] is given by

$$k_{FN,x} = \frac{(A_3)^{1/3} D^{2/3}}{1.786} \left\{ \frac{x^{-1/4}}{\left[1 - \left(x^{-1/2} + \frac{A_3}{A_4} x^{1/4}\right)^{-3/2} x^{-3/4}\right]^{1/3}} \right\} \tag{37}$$

The average mass transfer coefficient, $k_{FN,av}$, over an electrode of length L_e is given by

$$k_{FN,av} = \frac{1}{L_e} \int_0^{L_e} k_{FN,x} \, dx \tag{38}$$

Substitution of $k_{FN,x}$ from Equation 37 into Equation 38 and then integration [17] gives

$$k_{FN,av} = \frac{0.75 A_4 D^{2/3}}{L_e A_3^{2/3}} \left[\left(1 + \frac{A_3}{A_4} L_e^{3/4}\right)^{3/2} - 1\right]^{2/3} \tag{39}$$

Equation 39 shows that the dependence of $k_{FN,av}$ on L_e is very complex and is predominantly determined by the A_3/A_4 ratio.

5. Discussion

5.1. *Mass transfer to an electrode in the absence of gas evolution*

The working electrode consisted of nickel plate, 1 mm thick, which was placed against the back wall of the cell. Thus the velocity and mass transfer boundary layers develop simultaneously in the rectangular part of the cell compartment. The solution can be considered as a developing flow for $L_e/d_e < 12.5$, where d_e is the equivalent diameter of the cell compartment, and as a fully developed flow for $L_e/d_e \geqslant 12.5$ [18]. From the dimensions of the cell it can be calculated that $d_e = 0.013$ m at the level of the working electrode. Since the greatest electrode length is less than 12.5×0.013 m $= 0.163$ m, it can be concluded that a developing flow occurs in all experiments. For a laminar developing flow the average Sherwood number over an electrode of length L_e is given by [18, 19] as

$$Sh_{av} = 0.664 Re_{L_e}^{1/2} Sc^{1/3} \tag{40}$$

and for a turbulent developing flow as

$$Sh_{av} = 0.0366 Re_{L_e}^{0.8} Sc^{1/2} \tag{41}$$

Taking into account that $Sh_{av} = k_{av} L_e/D$, $Sc = \nu/D$ and $Re_{L_e} = v_s L_e/\nu$ it can be shown that, for a laminar developing flow,

$$k_{av} = 0.664 v_s^{1/2} L_e^{-1/2} \nu^{-1/6} D^{2/3} \tag{42}$$

and for a turbulent developing flow,

$$k_{av} = 0.0366 v_s^{0.8} L_e^{-0.2} \nu^{-0.3} D^{0.5} \quad (43)$$

Fig. 2 shows that at $L_e < 0.03$ m the slope of the log $k_{F,fi}$/log L_e is about -0.5. The slope indicates that, for $L_e < 0.03$ m, the solution flow behaves as a developing laminar flow. The change in the slope with increasing L_e may be caused by transition to a developing turbulent flow [19].

5.2. *Mass transfer to gas-evolving electrodes*

The models presented in Sections 4.1 and 4.2 also predict a decrease in k_{fi} with increasing electrode length. Since the theoretical relation for k_{fi} with combined forced and bubble-induced convection is very complicated, we first compare the theoretical and experimental results for bubble-induced convection alone.

From Equation 32 it follows that the theoretical slope of the log $k_{B,fi}$/log L_e curve is -0.25. This slope does not agree with the experimental slopes at both high and low current densities, namely 2.7 and 0.5 kA m^{-2}. The experimental slopes are about -0.7 at 0.005 m $\leqslant L_e \leqslant$ 0.02 m and about 0.0 at $L_e > 0.03$ m. It must be concluded that the model proposed in Section 4.1 does not describe mass transfer to a hydrogen-evolving electrode with bubble-induced convection sufficiently well. Ngoya [20] has proposed a mass transfer model similar to that given iin 4.2. Thus the Ngoya model is also not useful.

The shape of the log k_{fi}/log L_e for hydrogen-evolving electrodes differs completely from that of the log k_{fo}/log L_e relation for oxygen-evolving electrodes (Figs 3, 4). Fig. 3 shows that k_{fi} depends clearly on L_e at $L_e < 0.03$ m and Fig. 4 shows that k_{fo} is independent of L_e for the complete L_e range, namely from 0.005 to 0.16 m.

The models proposed in Sections 4.2 and 4.3 predict a dependence of the mass transfer coefficient of the indicator ion on the length of electrode; namely Equation 32 for a gas-evolving electrode with bubble-induced convection and Equation 39 for a gas-evolving electrode with combined forced and bubble-induced convection.

From these theoretical relations and the experimental results for oxygen-evolving electrodes it follows that the models proposed are not useful in describing the mass transfer of an indicator ion to an oxygen-evolving electrode. The experimental results for the oxygen-evolving electrodes fully support the convection-penetration model [4]. The mass transfer coefficient of $Fe(CN)_6^{3-}$ to a hydrogen-evolving electrode decreases with increasing length.

Fouad and Sedahmed [21] investigated the effect of hydrogen and oxygen evolution on the rate of mass transfer at vertical electrodes with a length from 0.025 to 0.5 m in a NaOH solution and in the absence of forced convection and with an electrode-diaphragm spacing of 0.04 m. They found that the dependence of the mass transfer coefficient of an indicator ion on the length of the electrode is very complex and is, moreover, a function of the current density.

The model for mass transfer in combined forced and bubble-induced flow is based on the separate relations for forced and for bubble-induced convection. Since the mass transfer with bubble-induced convection cannot be described by the proposed model and, moreover, the mass transfer in forced convection caused by pumping solution through the cell behaves as a developing laminar flow only for electrodes with $L_e < 0.03$ m, it is clear that Equation 39 is not useful for calculation of k_{FB} for a gas-evolving electrode in combined forced and bubble-induced flow.

Moreover, it can be concluded that at $i_H > 0.5$ kA m^{-2} the solution flow induced by rising bubbles does not behave as a laminar flow with streamlines parallel to the electrode surface. For a hydrogen-evolving electrode at a current density below about 0.01 kA m^{-2} the increase in k_{fi} is very sharp with increasing i_H [6]. Further research is necessary to determine the usefulness of the proposed models at very low rates of gas bubble evolution.

Various empirical correlations have been proposed to calculate k_{FN} from k_F and k_B [1], namely

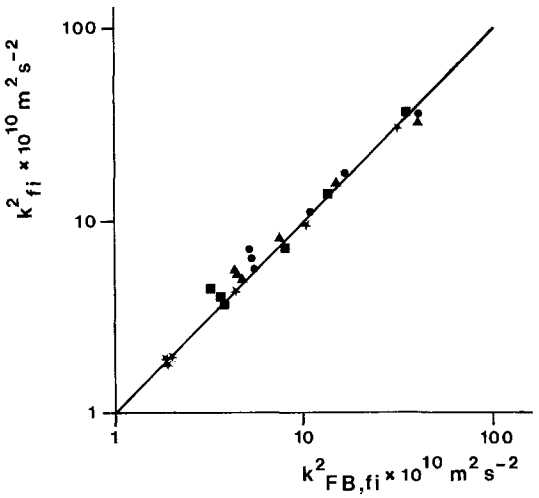

Fig. 7. The square of the experimental mass transfer coefficient of ferricyanide ions as a function of the square of the calculated mass transfer coefficient of ferricyanide ions on a double logarithmic scale for the electrodes of different length at two solution velocities and two current densities for hydrogen evolution.

$k_{FB} = k_F + k_B$ [22] and $k^2_{FB} = k^2_F + k^2_B$ [23]. From the experimental $k_{F,fi}$ (Fig. 2) and $k_{B,fi}$ (Fig. 5) we calculated $k_{FB,fi} = k_{F,fi} + k_{B,fi}$ at $v = 0.019$ and $0.16\,m\,s^{-1}$ and at $i_H = 0.5$ and $2.7\,kA\,m^{-2}$. Comparison of the calculated $k_{FB,fi}$ with the experimental k_{fi} (Fig. 3) showed that the simple addition of both mass transfer coefficients is unsuitable for obtaining the mass transfer coefficient with combined forced and bubble-induced convection. Birkett and Kuhn [24] have concluded that Beck's model is partially correct and of value in predicting and modelling industrial electrochemical processes

We also calculated $k^2_{FB} = k^2_F + k^2_B$ from the experimental results shown in Figs 2 and 5. The square of the experimental k_{fi} (Fig. 3) is plotted versus $k^2_{FB,fi}$ on a double logarithmic scale in Fig. 7 for two solution flow velocities and two current densities. From this figure it follows that the agreement between the experimental and the calculated mass transfer coefficients is satisfactory. Thus the relation $k^2_{FB} = k^2_F + k^2_B$ is suitable for calculation of the mass transfer coefficient in combined forced and bubble-induced convection from the single mass transfer coefficients.

References

[1] H. Vogt, in 'Comprehensive Treatise of Electrochemistry' (edited by E. Yeager, J. O'M. Bockris, B. E. Conway and S. Sarangapani) Plenum Press, New York and London (1983) pp. 6, 445.
[2] L. J. J. Janssen and E. Barendrecht, *Electrochim. Acta* **30** (1985) 683.
[3] L. J. J. Janssen and S. J. D. van Stralen, *ibid.* **26** (1981) 1011.
[4] L. J. J. Janssen and E. Barendrecht, *ibid.* **24** (1979) 693.
[5] L. J. J. Janssen and J. G. Hoogland, *ibid.* **18** (1973) 543.
[6] L. J. J. Janssen and E. Barendrecht, 'Dechema-Monographien Band 98', Verlag Chemie (1985) p. 463.
[7] C. R. Wilke, C. W. Tobias and M. Eisenberg, *Chem. Eng. Progr.* **49** (1953) 663.
[8] E. R. G. Eckert, 'Introduction to Heat and Mass Transfer', McGraw-Hill, New York, San Francisco, Toronto and London (1963) p. 186.
[9] B. E. Bongenaar-Schlenter, L. J. J. Janssen, S. J. D. van Stralen and E. Barendrecht, *J. Appl. Electrochem.* **15** (1985) 537.
[10] E. Gruber, 'Polymerchemie', UTB Steinhopff, Darmstadt (1980) p. 124.
[11] D. J. Pickett, 'Electrochemical Reactor Design', Elsevier Scientific, Amsterdam, Oxford, New York (1977) p. 125.
[12] W. H. McAdams, 'Heat Transmission', 2nd edn, McGraw-Hill, New York (1942) p. 217.
[13] J. Newman, 'Electrochemical Systems', Prentice-Hall, Englewood Cliffs, NJ (1973).
[14] A. Acrivos, *Chem. Eng. Sci.* **21** (1966) 343.
[15] J. Jorné, *J. Electrochem. Soc.* **131** (1984) 2283.
[16] E. R. G. Eckert and R. M. Drahe, 'Heat and Mass Transfer,' McGraw-Hill, New York (1959) p. 153.
[17] A. J. Geurts, private communication.
[18] D. J. Pickett and K. L. Ong, *Electrochim. Acta* **12** (1974) 875.
[19] D. J. Pickett, 'Electrochemical Reactor Design', Elsevier Scientific, Amsterdam (1977) p. 139.
[20] F. N. Ngoya, *Electrochim. Acta* **28** (1983) 1865.

[21] M. G. Fouad and G. H. Sedahmed, *ibid.* **17** (1972) 665.
[22] S. S. Kutateladze, *Int. J. Heat Mass Transfer* **4** (1961) 31.
[23] T. R. Beck, *J. Electrochem. Soc.* **116** (1969) 1038.
[24] M. D. Birkett and A. Kuhn, *Electrochim. Acta* **22** (1977) 1427.